

## Transverse mode imaging of guided matter waves

R. G. Dall, S. S. Hodgman, M. T. Johnsson, K. G. H. Baldwin, and A. G. Truscott\*

*ARC Centre of Excellence for Quantum-Atom Optics and Research School of Physics and Engineering, Australian National University, Canberra, ACT 0200, Australia*

(Received 1 May 2009; published 7 January 2010)

Ultracold atoms whose de Broglie wavelength is of the same order as an extended confining potential can experience waveguiding along the potential. When the transverse kinetic energy of the atoms is sufficiently low, they can be guided in the lowest order mode of the confining potential by analogy with light guided by a single mode optical fiber. We have obtained the first images of the transverse mode structure of guided matter waves in a confining potential with up to 65% of atoms in the lowest order mode. The coherence of the guided atomic de Broglie waves is demonstrated by the diffraction pattern produced when incident upon a two dimensional periodic structure. Such coherent waveguides will be important atom optic components in devices with applications such as atom holography and atom interferometry.

DOI: [10.1103/PhysRevA.81.011602](https://doi.org/10.1103/PhysRevA.81.011602)

PACS number(s): 03.75.Pp, 03.75.Nt, 67.85.Jk

Establishing the mode structure transmitted by optical fibers is important in applications ranging from telecommunications to laser gyroscopes. In the work reported here, we transmit atomic de Broglie waves through a waveguide formed by a focused laser beam and determine the mode structure by directly imaging the atomic density distribution after it leaves the waveguide in the plane transverse to the laser beam.

The new information provided by two dimensional imaging enables direct measurement of the transverse matter-wave density distribution to elucidate the atomic beam properties, including the mode occupancy of the de Broglie waveguide. The ability to determine and control the mode structure of guided matter waves will be important in future applications such as atom interferometry.

Early atom guiding experiments focused on the transmission properties of thermal atoms through hollow [1,2] and (more recently) microstructured [3,4] optical fibers, as well as magnetic guiding structures [5,6]. However, the large kinetic energy of thermal atoms results in highly multimode excitation of the discrete transverse energy levels in the guiding potential. The use of ultracold atoms reduces the excitation energy, and Bose-Einstein condensates (BECs) were later coupled into guiding structures employing optical [7], magnetic [8], and dressed-state rf potentials [9].

More recently, the guiding of atom laser beams output-coupled from BECs has been achieved using optical waveguides to confine  $^{87}\text{Rb}$  atoms released from magnetic [10] and optical [11] trapping fields. In both cases the output-coupled atoms were confined by far-red-detuned, focused laser beams aligned horizontally. The significance of these experiments is that the output-coupling mechanism allows the population of just a few transverse modes, with  $\sim 14\%$  [10] and  $\sim 50\%$  [11] in the transverse ground state. (More recently the second group has reported  $\sim 85\%$  ground state mode occupancy [12].) The mode population was inferred by observing the propagation of atoms along the waveguide via absorption imaging, which also enables the transverse energy of the guided atoms to be determined and compared with that expected for various transverse mode combinations.

Unlike these earlier experiments, we have been able to directly image the transverse mode structure of the guided matter waves by taking advantage of the high detection efficiency which is characteristic of metastable helium ( $\text{He}^*$ ) atoms [13]. Our detector consists of a microchannel plate (MCP) backed by a phosphor screen which generates a fluorescence spot each time a  $\text{He}^*$  atom strikes the MCP. A CCD camera then images the resulting fluorescence from the phosphor. We are able to observe end-on to the guiding structure the transverse spatial profile of the atoms as they strike the detector, thereby allowing direct measurement of the guided matter-wave mode structure.

The experiment consists of our existing magnetically trapped  $\text{He}^*$  BEC apparatus [14] with the addition of an optical dipole trap and guide (Fig. 1). We trap and cool the atomic sample to just above the BEC transition point in the magnetic trap before adiabatically transferring the atoms to the optical dipole trap created by focusing a 50 mW red-detuned (1550 nm) laser beam to a  $1/e$  diameter of  $\sim 30 \mu\text{m}$ . The optical trap produces a weak axial trapping frequency of 22 Hz, and strong radial trapping frequencies of 1075 and 1500 Hz, because the focused spot is slightly elliptical. A condensate comprising a few hundred thousand atoms is formed automatically in the dimple potential created by the laser. Figure 1(a) shows an image of the BEC after the optical trap is switched off and the atoms fall under gravity onto the MCP located  $\sim 18$  cm below. The initial transverse velocities of the atomic ensemble are determined by mutually repulsive “mean-field” interactions occurring before and during release from the trap. The result is a rapidly divergent atomic cloud that produces a large ( $\sim 1$ -cm diameter) image.

By comparison, Fig. 1(b) shows an end-on profile of our  $\text{He}^*$  atom laser produced by rf outcoupling  $\text{He}^*$  atoms from the magnetic trap. The mode profile of a freely propagating atom laser beam is itself far from an ideal Gaussian, again because of mean-field interactions that generate “caustics” [15] and interference fringes [16,17]. Attempts to improve the atom laser beam profile by Raman outcoupling [18] increase the collimation of the beam through photon momentum transfer in the atom laser propagation direction due to the Raman process, which has the added benefit of reducing the interaction time of the outcoupled atoms with the BEC. However, even under

\*andrew.truscott@anu.edu.au

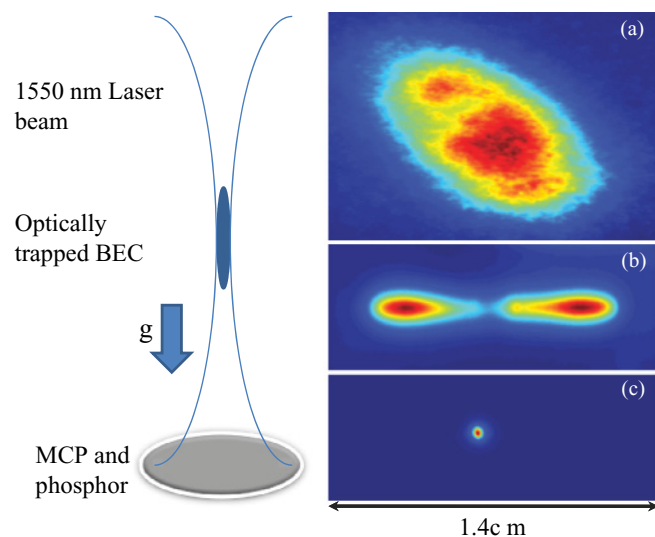


FIG. 1. (Color online) Experimental schematic. The BEC is formed in an all-optical trap at the focus of a single laser beam. Atoms outcoupled from the BEC by reducing the laser intensity create an atom laser beam that is optically guided toward the MCP detector located  $\sim 18$  cm below. (a) Image formed by dropping the BEC onto the MCP without guiding. (b) Atom laser image generated by rf outcoupling atoms from a magnetic trap followed by free expansion onto the detector below. (c) Guided atom laser image produced by adiabatically lowering the optical trapping potential. Note: images taken with different MCP gain values.

such circumstances beam divergence can still occur, and the beam quality is not completely ideal [18].

To improve the atom laser beam profile, instead of rf or Raman outcoupling, we slowly lower the laser intensity until gravity overcomes the trapping potential at the bottom of the condensate, allowing atoms to leak out into the optical waveguide. A similar technique was used by Cennini *et al.* [19] to create an atom laser. However, the trapping laser propagated horizontally such that outcoupled atoms freely expanded after falling vertically out of the optical trap. In our experiment, the trapping laser propagates vertically, such that only the weak axis of the optical potential opposes gravity. Atoms released from the optical trap are subsequently radially confined by the strong axis of the optical potential and are thereby guided.

As the outcoupling process can be made adiabatic, it is expected that atoms in the ground state of the optical trap (i.e., the BEC) will be transferred into the ground state (lowest order transverse mode) of the waveguide. The atoms then fall under gravity until the radial confinement relaxes due to the expansion of the laser beam, which also results in transverse adiabatic cooling of the guided atoms. Once the atoms are no longer guided, they simply expand ballistically in the transverse direction.

In detail the outcoupling process is as follows: After condensate formation, the laser power of the dipole trap is linearly ramped from 50 to 22 mW over 100 ms to outcouple only the thermal atoms into the guide, leaving a nearly pure condensate in the trap. The laser power is then held constant for 200 milliseconds to allow the condensate to stabilize and to separate in time the outcoupled thermal and atom laser beams on the detector. Finally the laser power is ramped from

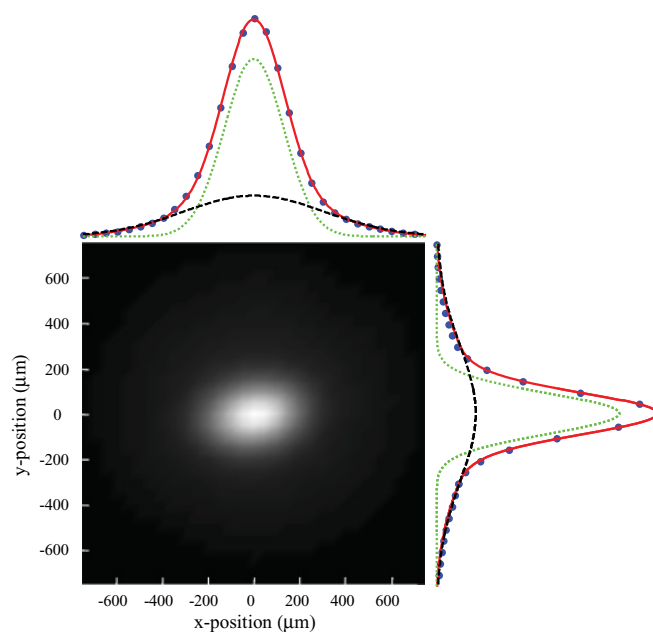


FIG. 2. (Color online) Magnified image of the guided atom laser. Cross section profiles are shown adjacent to their corresponding axes with the solid line being a least squares fit to the experimental data points ( $50 \mu\text{m}$  pixels). The two-component Gaussian fit comprises a dotted line attributed to the fundamental mode, while the dashed line is attributed to the sum of higher-order thermal modes.

22 to 19 mW over 100 ms, adiabatically transferring the entire condensate from the trap into the single mode of the guide.

The image of the transverse mode profile from our guided atom laser beam is shown in Fig. 1(c). The guided atom laser beam diameter is much smaller than the unguided atom laser [Fig. 1(b)]. This results in an increase in the intensity of  $\text{He}^*$  atoms of more than two orders of magnitude, which requires that the gain of the MCP be reduced significantly to avoid saturation.

Figure 2 shows an expanded view of Fig. 1(c), with least squares fits to the image profile. The fitting function comprises two Gaussians, the narrowest of which we attribute to the lowest order mode of the optical potential where the atoms are strongly guided, whereas the wider is attributed to the sum of higher order modes. At finite temperatures a thermal component is always present in the condensate, and it is therefore expected that some additional modes will be thermally populated in the waveguide.

The two Gaussian components provide an excellent fit to the data in Fig. 2, where a point-spread function accounts for the finite resolution of our detection system ( $\sim 100 \mu\text{m}$ ). The  $1/e$  diameter for the two orthogonal axes of the lowest order mode are  $260$  and  $360 \mu\text{m}$ . This compares well, within experimental uncertainties (including absolute knowledge of the optical potential and detector resolution), to the theoretical model predictions (below) of  $280$  and  $340 \mu\text{m}$ , respectively. By integrating the two Gaussian fit functions, the fraction of atoms in the fundamental mode of the guided region was determined to be  $65\%$ , compared with previously reported values of  $14\%$  [10],  $50\%$  [11], and  $85\%$  [12].

The theoretical values for the widths of the atom laser beam at the detector were obtained by carrying out a numerical

simulation of the guiding experiment using the Gross-Pitaevskii (GP) equation. The initial outcoupling process, where the vertical trapping potential was lowered until atoms spill out of the trap under the influence of gravity, was simulated in two dimensions in a region extending from the condensate down to a point 2-mm below. Because the waist and divergence of the optical beam differed in the tight and weak directions, this two dimensional simulation was carried out twice: once in the  $x, z$  plane and once in the  $y, z$  plane, where  $z$  was the direction of gravity, and where  $x$  and  $y$  were the tight and weak trapping axes of the guide beam.

Specifically, the Hamiltonian used for this initial part of the simulation in the  $x, z$  plane was given by

$$\hat{H} = \iint \hat{\Psi}^\dagger \left( -\frac{\hbar^2 \nabla^2}{2M} + V_{\text{trap}}(t) + mgz \right) \hat{\Psi} dx dz + \frac{U}{2} \iint \hat{\Psi}^\dagger \hat{\Psi}^\dagger \hat{\Psi} \hat{\Psi} dx dz, \quad (1)$$

where  $\hat{\Psi}(x, z, t)$  is the operator for the atomic field,  $U = 4\pi\hbar^2 a/m$  is the nonlinear interaction strength, and  $a$  is the  $s$ -wave scattering length of the atoms.

The potential depth was calculated from the experimental parameters by using [20]

$$V_{\text{trap}} = \frac{3\lambda^3 \Gamma}{16\pi^2 c \Delta} I(\mathbf{r}, \mathbf{t}), \quad (2)$$

where  $\lambda$  is the wavelength of the trapping laser,  $\Delta$  is the detuning,  $\Gamma$  is the decay rate of the excited atomic level, and  $I$  is the intensity of the trapping laser.

The GP equation corresponding to the Hamiltonian (1) is

$$i\hbar \frac{d}{dt} \psi = \left[ -\frac{\hbar^2 \nabla^2}{2m} + V_0(x, z, t) + U |\psi|^2 \right] \psi, \quad (3)$$

where  $\psi(x, z, t)$  is now the order parameter of the condensate and as such carries information on density and phase but not on the quantum statistics of the system. Equation (3) was solved numerically using the open source package XMDS [21].

An absorbing boundary condition was applied at the lower edge of the simulation region, allowing us to run the simulation until initial outcoupling transients died away and steady state was achieved. We then extracted a one-dimensional horizontal slice 1.85-mm below the condensate and took this as the transverse wave function of the atom laser beam. To examine whether the beam was in the transverse ground state of the guide at this point, we carried out energy minimization, imaginary time simulations to find the ground state of the atoms in the guide at this height, and compared it to the transverse state of the atomic beam given by our simulations. This showed that the atom laser was in the ground state to within 1% at this point, in both the tight and weak trapping directions, confirming that the outcoupling process was adiabatic. To model the subsequent evolution of the atom laser beam from 1.85-mm below the condensate to the detector 187.2-mm below, we carried out a one-dimensional GP simulation of the transverse wave function, with a time-dependent confining potential mimicking the optical potential that the atoms would experience as they fall to the detector. This process was carried out for both the tight and weak trapping axes of the optical potential.

It is instructive to compare these profiles with the width of the ground state of the guiding potential at the detector. Again using an imaginary time approach we find that the transverse ground state of the atom laser is essentially Gaussian, because of the nearly harmonic nature of the guide so far from the focus, with  $1/e$  values of 381 and 435  $\mu\text{m}$  in the weak and tight optical trapping directions, respectively.

The fact that the observed atom laser profile is narrower than the ground state of the optical guide beam at the detector is resolved by noting that the guiding is not adiabatic through the entire fall distance. As mentioned above, during the outcoupling process and the initial part of the fall, the optical potential is strong enough to ensure that the transverse wave function of the atoms adiabatically follows the guiding potential, and the atoms remain in the ground state of the guide. As the atoms fall, however, their velocity increases and the optical beam diverges, resulting in a weaker potential and breakdown of adiabaticity criteria. Consequently, the atoms no longer adiabatically follow the optical potential, resulting in a component of free space expansion.

The speed of this expansion depends on how tightly confined the atom beam is when it begins to escape the guide. Momentum uncertainty dictates that the tighter the confinement, the more rapid the expansion. For example, if the atoms were to be completely free of the potential 2-mm below the condensate and allowed to freely expand, the resulting detector image would have  $1/e$  values of 429 and 485  $\mu\text{m}$ . In our experiment, however, atoms are strongly guided to a point further down, by which time the atom beam has widened to a point where the transverse momentum uncertainty is much smaller. The initial adiabatic guiding followed by the nonadiabatic free-space evolution results in an atomic beam profile at the detector that is much narrower than that of atoms in the ground state of the potential created by the optical guide beam.

To study the coherence properties of the guided atom laser beam we perform a diffraction experiment using a two-dimensional transmission grating. The grating consists of a commercial foil with 2- $\mu\text{m}$  diameter holes at 4- $\mu\text{m}$  centers in a square grid pattern (Quantifoil 2/2) located  $\sim 12$  cm below the condensate and  $\sim 6$  cm above the detector.

Figure 3(a) shows the resulting interference image produced by the guided atom laser at the detector. A fringe

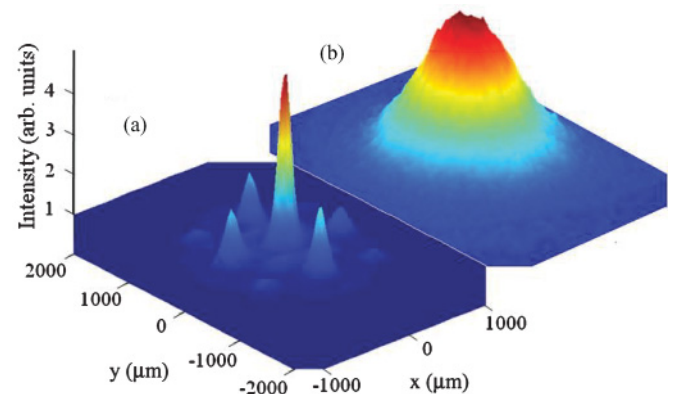


FIG. 3. (Color online) Diffraction images (three-dimensional surface plots) from the MCP for the (a) guided condensate beam and (b) guided thermal beam.

visibility of  $\sim 91\%$  was observed, which demonstrates the coherence of the guided atom laser and is consistent with the guided beam being predominately in the fundamental mode. The separation of the diffraction orders was within 10% of that expected from the diffraction equation for atomic de Broglie waves accelerated under gravity to the grating position. For comparison, the image produced by solely thermally populated modes (i.e., no condensate component) is shown in Fig. 3(b); as expected, no interference is observed.

In summary, we have obtained the first images of the transverse profile of a guided atom laser beam. Approximately 65% of the atoms are guided in the fundamental mode whose beam diameter is consistent with theoretical modeling. We have shown that guiding the atom laser beam results in a smooth Gaussian mode profile, avoiding the formation of structure that is often present in atom laser beams. Compared to the free expansion of an atom laser outcoupled from our magnetic trap, we have shown that the atom guide increases the intensity of the atom laser by several orders of magnitude.

Finally, we have demonstrated the coherence of the guided atom laser as evidenced by the high visibility interference pattern generated from a transmission diffraction grating.

The present waveguiding configuration, combined with improved He\* single atom detection, will also enable the measurement of the quantum statistical properties of the guided matter waves. Analogously with the Hanbury-Brown and Twiss experiments conducted elsewhere [22], we aim to determine the second (and perhaps higher) order correlation functions of guided atoms by implementing a new detector with the necessary spatial and temporal resolution that we are currently developing. The ability to alter the mode occupancy should then allow a quantum statistical study of the transition from a thermal to a coherent source of guided matter waves.

R.G.D., M.T.J., and A.G.T. would like to acknowledge the support of the Australian Research Council Centre of Excellence for Quantum-Atom Optics. M.T.J. also acknowledges support from the Australian NCI Supercomputing Facility.

- 
- [1] M. J. Renn *et al.*, Phys. Rev. Lett. **75**, 3253 (1995).
  - [2] R. G. Dall, M. D. Hoogerland, K. G. H. Baldwin, and S. J. Buckman, J. Opt. B **1**, 396 (1999).
  - [3] T. Takekoshi and R. J. Knize, Phys. Rev. Lett. **98**, 210404 (2007).
  - [4] C. A. Christensen *et al.*, Phys. Rev. A **78**, 033429 (2008).
  - [5] J. Fortagh, A. Grossman, C. Zimmermann, and T. W. Hänsch, Phys. Rev. Lett. **81**, 5310 (1998).
  - [6] J. Denschlag, D. Cassettari, and J. Schmiedmayer, Phys. Rev. Lett. **82**, 2014 (1999).
  - [7] K. Bongs *et al.*, Phys. Rev. A **63**, 031602(R) (2001).
  - [8] A. E. Leanhardt *et al.*, Phys. Rev. Lett. **89**, 040401 (2002).
  - [9] S. Hofferberth, I. Lesanovsky, B. Fischer, J. Verdu, and J. Schmiedmayer, Nature Physics **2**, 710 (2006).
  - [10] W. Guerin *et al.*, Phys. Rev. Lett. **97**, 200402 (2006).
  - [11] A. Couvert *et al.*, Europhys. Lett. **83**, 50001 (2008).
  - [12] G. L. Gattobigio, A. Couvert, M. Jeppeson, R. Mathevet, and D. Guéry-Odelin, Phys. Rev. A **80**, 041605(R) (2009).
  - [13] K. G. H. Baldwin, Contemp. Phys. **46**, 105 (2005).
  - [14] R. G. Dall and A. G. Truscott, Opt. Commun. **270**, 255 (2007).
  - [15] J.-F. Riou *et al.*, Phys. Rev. Lett. **96**, 070404 (2006).
  - [16] T. Busch, M. Köhl, T. Esslinger, and K. Mølmer, Phys. Rev. A **65**, 043615 (2002).
  - [17] R. G. Dall *et al.*, Opt. Express **15**, 17673 (2007).
  - [18] M. Jeppesen, J. Dugué, G. R. Dennis, M. T. Johnsson, C. Figl, N. P. Robins, and J. D. Close, Phys. Rev. A **77**, 063618 (2008).
  - [19] G. Cennini, G. Ritt, C. Geckeler, and M. Weitz, Phys. Rev. Lett. **91**, 240408 (2003).
  - [20] R. Grimm, M. Weidemüller, and Y. B. Ovchinnikov, Adv. At. Mol. Opt. Phys. **42**, 95 (2000).
  - [21] XMDS documentation and source code available from [www.xmnds.org](http://www.xmnds.org).
  - [22] T. Jeltes *et al.*, Nature (London) **445**, 402 (2007).